ARTICLE

Check for updates

Diamonds, dunites, and metasomatic rocks formed by melt/rock reaction in craton roots

Zsanett Pintér [1,2,3 ✉], Stephen F. Foley [1,2] & Gregory M. Yaxley [2]

The thick mantle lithosphere beneath cratons consists of strongly reduced rocks that have reacted with oxidized melts. These low-silica, incipient melts are rich in CO_2 and H_2O and react with surrounding rocks forming an enriched zone at the base of the lithosphere, which is the source region for many diamonds. Here, we reproduce these reactions in novel experiments in which oxidised, hydrous carbonate-rich melts are reacted with reduced, depleted peridotite at 5 GPa pressure. Results explain several key features of the mantle sample in kimberlites as products of a single process, namely the formation of diamonds, phlogopite and alkali-amphibole bearing rocks, iron-rich dunites, and garnets and clinopyroxenes with pyroxenitic compositions. Initially, redox freezing occurs where melts meet the reduced peridotite, depositing diamonds and associated garnet and clinopyroxenes. The spreading reaction front leaves behind Fe-rich dunite, and crystallizing phlogopite and amphibole when the melt solidifies at the reaction front.

[1] School of Natural Sciences and ARC Centre of Excellence for Core to Crust Fluid Systems, Macquarie University, North Ryde, NSW, Australia. [2] Research School of Earth Sciences, Australian National University, Canberra, ACT, Australia. [3] School of Earth, Atmosphere and Environment,, Monash University, Melbourne, VIC, Australia. ✉email: zsanett.pinter@monash.edu

The thick mantle lithosphere beneath the cratons—the ancient cores of the continents—has cold, stable roots reaching ~250 km depth. The cratonic lithosphere suffered extensive melting during Earth's early history, resulting in strong depletion in alkali elements (Na, K), basaltic components (Ca, Ti, Fe, Al), and volatiles (H_2O, CO_2), along with enrichment in Mg, Ni, and Cr[1]. The residue consists of dunite and harzburgite containing Mg-rich garnet or spinel and formed stable and thick lithosphere, the lower parts of which are referred to as cratonic roots. The redox state, or oxygen fugacity (fO_2), of the lithospheric mantle, is expressed by the distribution of Fe^{3+} between spinel, garnet, and pyroxenes, and decreases systematically with increasing pressure through unmetasomatized cratonic lithospheric mantle[2]. Diamonds may be stabilized at depths greater than ~130 km along the cold geotherms typical of cratonic roots[1].

Investigations of cratonic mantle xenoliths—fragments of the mantle brought to the surface by kimberlite magmas—have revealed that cratonic roots have been strongly modified by transformation into new mineral and rock assemblages (known as mantle metasomatism) caused by the crystallization of, and reaction with melts that infiltrated from the convecting mantle below[3–5], as well as remelting of these metasomatized rocks. These xenoliths indicate strong changes in major- and trace-element compositions, frequently resulting in enrichment in clinopyroxene and garnet[3,6], or in the crystallization of the hydrous minerals phlogopite and alkali amphiboles, Ti-oxides, and other accessory phases[3,4,7]. Carbonates are remarkably rarely sampled in cratonic roots compared to diamond[5], which is an expression of the low fO_2 conditions[8]. The compositions of infiltrating, metasomatic melts must vary to cause the observed range of secondary mineral assemblages. Clinopyroxene-rich, olivine-bearing rocks (wehrlites) are associated with CO_2-rich silica-undersaturated mafic melts[9], whereas mica pyroxenites and MARID (mica-amphibole-rutile-ilmenite-diopside) xenoliths have been linked to potassium-rich hydrous, but carbon-poor melts[7,10,11].

The ancient and long-lived cratonic roots are characterized by low geothermal gradients[1], along which peridotites do not melt except in rare circumstances. Well below the craton, melting may occur as asthenospheric peridotite containing carbon in reduced forms (e.g., diamond, methane-fluid) upwells and encounters progressively more oxidizing conditions. Diamond or methane may oxidize to carbonates and water, depressing the melting point by 300–500 °C[12] (the 'oxidized solidus'[12,13]) below the base of cratonic roots (Fig. 1). Only a small amount of melt is present over a wide temperature interval until major melting occurs (Fig. 1), giving ample opportunity for these incipient melts to modify the craton roots. In this incipient melting regime at pressures of 4–7 GPa (130–220 km depth), melting of peridotites produces melts ranging in composition from alkali-rich hydrous carbonate melts containing <10% SiO_2 (carbonatites) to carbonated silicate melts with 20–30% SiO_2 (the most similar melts seen at the surface are ultramafic lamprophyres)[13,14]. Experiments have shown that the exact type of melt depends on the fertility of the peridotite and on the degree of melting, with carbonatite melts more likely emanating from enriched peridotites and low degrees of melting[13–15] because melt compositions are mainly controlled by the breakdown of volatile-bearing minor phases such as carbonate and phlogopite. When these melts encounter the reduced cratonic root, they will freeze because the reduced solidus is located at 150–250 °C higher temperatures, depending on the ratio of C to H_2O present[12,16] (Fig. 1), a process known as redox freezing[16,17]. The reduced melting curve lies above the typical conductive geothermal gradient for the cratonic lithospheric mantle (Fig. 1A), so that melting would be exceptionally uncommon in the reduced peridotite of the cratonic roots. This reduced and relatively cool zone will therefore act as a trap for melts in which infiltrating oxidized melts cause metasomatism of the pre-existing rocks (Fig. 1B). Continued infiltration may gradually oxidize the craton roots until discrete carbonate-bearing rocks are stabilized, most likely in dykes. However, these are hardly ever represented amongst the xenolith population[4,5], presumably, because they are the first to melt when re-heated (Fig. 1B) and so contribute to later melts rather than being sampled as xenoliths. The majority of sampled diamonds originate from the base of the cratonic lithosphere at temperatures of 1140–1170 °C and pressures of 5.0–6.1 GPa[18,19], within the redox freezing zone in Fig. 1A.
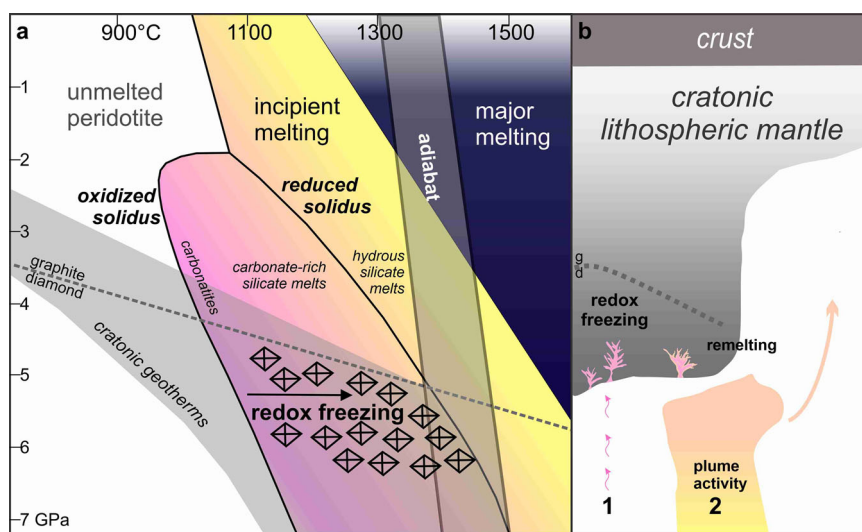

Fig. 1 Incipient melts in lower cratonic settings. a Melting curves of peridotite in oxidized and reduced conditions in the incipient melt regime. Oxidized melts freeze in the reduced lithosphere, depositing diamonds as the local solidus increases in temperature as it evolves from a carbonate solidus to a reduced solidus (black arrow). The region of diamond formation is marked with diamond symbols[18,19]. Pink and peach areas indicate carbonatitic, and carbonate-rich silicate melt; yellow areas have hydrous silicate melts. Dashed line: graphite-diamond boundary[46]. Cratonic geotherms (35–45 mW/m² [47,48]). Temperature range of mantle adiabat based on mantle potential temperatures of 1300–1400 °C. **b** schematic relationship of the cratonic lithosphere and incipient melt metasomatism. 1: the gradual influx of carbonate-rich incipient melts freezes in the base of the cratonic lithosphere, depositing diamonds by redox freezing[8,17]. 2: Later reheating of the lowermost metasomatized cratonic lithosphere induces re-melting of the metasomatized rocks[8].
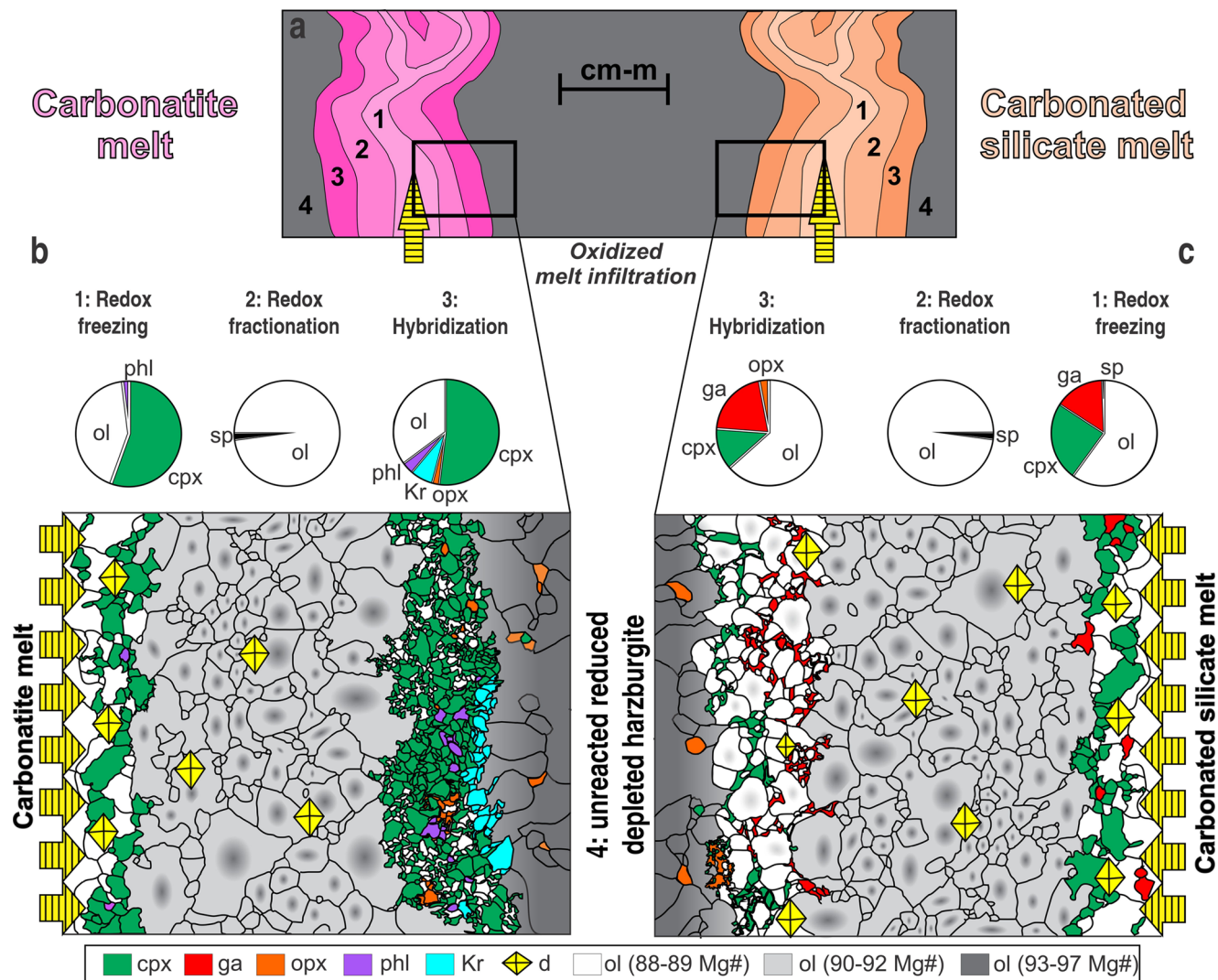
Fig. 2 Experimental results showing the effects of incipient melt infiltration into reduced, peridotite. a Stylized reaction zones resulting from redox freezing, reactive melt infiltration, and hybridization by carbonatite **b** and carbonated silicate incipient melts **c** (based on microprobe maps, see Suppl. Figs. 3 and 4). Modal proportions in each reaction zone are illustrated as pie charts highlighting the modal enrichment in clinopyroxene and other silicate minerals. Silicate phases are shown in colors (see key at bottom). Yellow diamond symbols represent (metastable) graphite precipitation in experiments (equivalent to diamonds in the lower lithosphere).

Results and discussion

Dynamic metasomatism experiments. To experimentally simulate the processes that arise from redox freezing between oxidized, low-degree melts and reduced, depleted cratonic lithosphere, we selected a harzburgite composition to represent the unmodified cratonic root and reacted this in separate experiments with two representative oxidized melts (see Methods). A crucial feature of the current experiments is the establishment of a redox contrast between the oxidized melts and the reduced peridotite to reproduce the conditions likely to prevail during infiltration of carbonate-rich melt into the lower lithosphere, causing the reduction of the carbonate component $(CO_3)^{2-}$ in the melt to elemental carbon (graphite/diamond) by redox freezing. To achieve this, Fe capsules were used (see Supplementary Note 2), in contrast to previous experiments that were conducted in more oxidized conditions consistent with carbonate stability[20,21]. In the Fe capsules, the oxygen fugacity in the experiments was buffered at the iron–wüstite buffer (IW). Whilst the cratonic lithospheric mantle at 5 GPa is likely not as strongly reduced as IW, this is not important—we simply seek to establish a redox contrast between the reduced peridotite and the oxidized carbonate melt compositions.

The two oxidized melt compositions were selected from previous experimental studies[13,14] to represent the range of low-degree melts that form by melting of peridotite with both CO_2 and H_2O at similar pressure-temperature conditions (5 GPa, ~1140–1150 °C). Melts range from an alkali-rich hydrous carbonatitic melt (<10 wt% SiO_2) at low degrees of melting (hereafter referred to as 'carbonatite melt', Fig. 2) to an alkali-poorer, CO_2–H_2O-bearing carbonated silicate melt (20–30 wt% SiO_2) with a composition similar to natural ultramafic lamprophyres (hereafter 'carbonated silicate melt', Fig. 2) (see Methods).

Two experiments were conducted in gold capsules in more oxidized conditions similar to earlier experiments[20,21]: the oxygen fugacity of these experiments is not buffered but is high enough to maintain the stability of carbonate. These had high proportions of melt to circumvent the difficulty of finding the products of the reaction: carbonate-rich melts have low viscosity and are highly mobile at low melt fractions, so evidence of reaction with the peridotite may be challenging to observe. These experiments confirm the observation from earlier studies[20–23], that carbonatitic melt consumes orthopyroxene in the peridotite and may crystallize garnet[20], clinopyroxene[21], and magnesite[20]. Only small
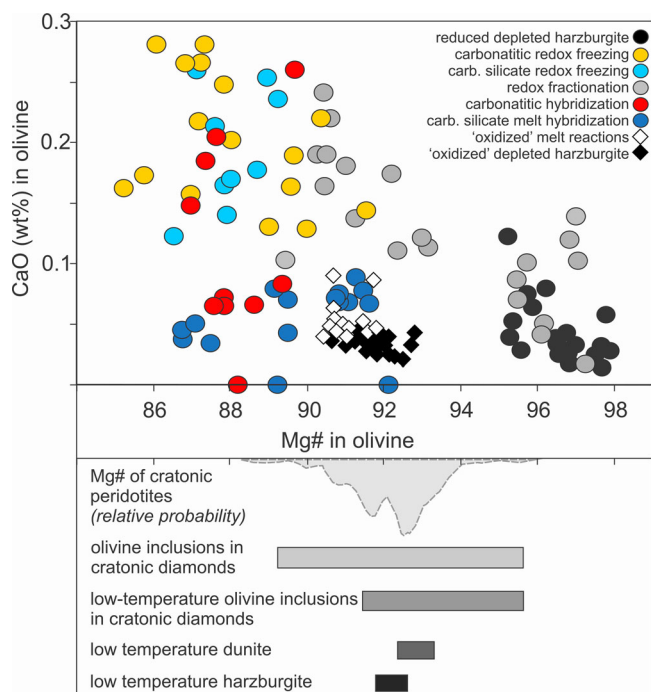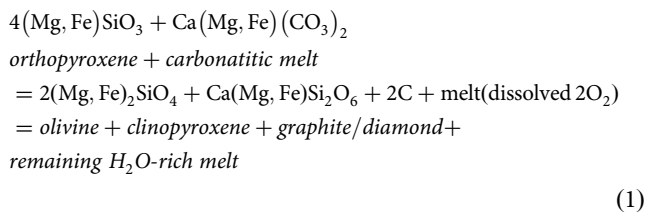
Fig. 3 CaO content versus Mg# of the olivines from the redox freezing, redox fractionation, and hybridization zones. Low temperature cratonic dunites and harzburgites[33], diamond inclusions[41].

chemical changes are observable in the harzburgite wall rock: alkalies do not form new, distinct phases, but are carried further in the carbonatitic melt[20,21]. These experiments in gold capsules serve to confirm the similarity to previous experiments and to emphasize the contrast to the experiments in Fe metal capsules.
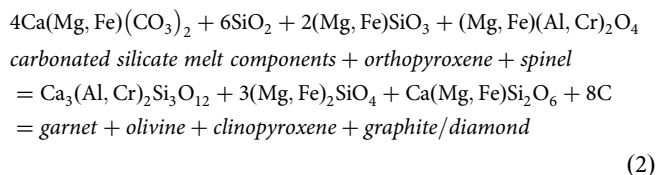
Redox reactions between oxidized melts and reduced harzburgite in the experiments in Fe capsules yield three distinct zones of contrasting mineralogy (Fig. 2), showing differences according to the oxidized melt compositions. Characteristics and natural analogs of these reaction zones are described here as the *redox freezing zone*, the *redox fractionation zone*, and the *hybridization zone*.

The redox freezing zone: deposition of diamonds. *Redox freezing* occurs at the first contact of oxidized melts with the reduced, depleted harzburgite. Here the modal proportion of clinopyroxene increases in the reaction zone (Fig. 2—left, 2B, zone 1; further details in Supplementary Notes 3 and 4) as the carbonatitic melt reacts with orthopyroxene in the harzburgite. Diopsidic clinopyroxene, more iron-rich olivine (Mg# 88.1, Fig. 3), and graphite form via Reaction (1) (simplified as end members). K_2CO_3 and H_2O in the melt is accommodated by the formation of small amounts of phlogopite, again involving dolomite melt components reacting with enstatite and Mg-Tschermaks components in primary orthopyroxene.

$$4(Mg, Fe)SiO_3 + Ca(Mg, Fe)(CO_3)_2$$
orthopyroxene + carbonatitic melt
$$= 2(Mg, Fe)_2SiO_4 + Ca(Mg, Fe)Si_2O_6 + 2C + melt(dissolved\ 2O_2)$$
$$= olivine + clinopyroxene + graphite/diamond +$$
remaining H_2O-rich melt

$$(1)$$

Reaction with the carbonated silicate melt (Fig. 2 right, 2C, zone 1) yields a similar modal increase in clinopyroxene and the formation of iron-richer olivines, but here grossular-rich garnet is

also stabilized by the redox freezing reaction (Reaction (2), Fig. 4A), reflecting the higher initial SiO_2 and Al_2O_3 contents of the melt. Spinel in the harzburgite is mostly consumed in the redox freezing zone, with its components entering clinopyroxene, olivine and garnet (Reaction (2)). Phlogopite was not detected as the K_2O abundance in the carbonated silicate melt is much lower.

$$4Ca(Mg, Fe)(CO_3)_2 + 6SiO_2 + 2(Mg, Fe)SiO_3 + (Mg, Fe)(Al, Cr)_2O_4$$
carbonated silicate melt components + orthopyroxene + spinel
$$= Ca_3(Al, Cr)_2Si_3O_{12} + 3(Mg, Fe)_2SiO_4 + Ca(Mg, Fe)Si_2O_6 + 8C$$
$$= garnet + olivine + clinopyroxene + graphite/diamond$$

$$(2)$$

In both reactions (Fig. 2), the (CO_3^{2-}) carbonate component is reduced to elemental carbon, and orthopyroxene is replaced by clinopyroxene and Fe-rich olivine[9]. In cratonic roots, these reactions take place in the diamond stability field, so that diamond will form during redox freezing. If diamonds trap inclusions during growth, these are likely to be the other products of the redox freezing reactions. The experiments indicate that redox freezing of alkali-rich hydrous carbonatitic melts can produce a suite of mineral inclusions similar to diopsidic clinopyroxenes of fertile lherzolites (Fig. 4B) and olivines with Mg# 85–91 (Fig. 3).

Experimental garnets from the redox freezing zone contain low Cr_2O_3 (1.2–3.06 wt%, Fig. 4B) and high CaO, and resemble garnet compositions that have been classified as eclogitic–wehrlitic[22]. In nature, cratonic peridotite assemblages do not contain these anomalously Ca-rich garnets, however, they are similar to garnets from 'Type C' eclogites (Fig. 4A), which occur as xenoliths from various cratons[22,24]. During the experimental redox freezing process, the carbonated silicate melt reacted with minor Cr-bearing spinel and clinopyroxene originally in the harzburgite, forming Cr-bearing garnet and clinopyroxene. In nature, redox freezing processes could lead to two strikingly different Ca-rich garnet populations depending on the melt/rock ratio. At high melt/rock ratios, melt could metasomatize the harzburgitic rock section affecting all the modal mineralogy. Depending on the initial Cr_2O_3 of harzburgitic garnet, exotic Ca-rich garnets with variable Cr (e.g., kimberlite-hosted wehrlitic xenoliths field[25,26] on Fig. 4B[25]) could form. Fertile, Cr-poor peridotites are more likely to retain low Cr contents, whereas Cr-rich depleted peridotites would inherit high Cr contents during redox freezing. However, at low melt/rock ratios, the interaction of melt may be localized, reacting only with the major Cr-poor phases such as olivine (<0.1 wt%) and orthopyroxene (<0.3 wt%). In this case, redox freezing could lead to the formation of Ca-rich, yet Cr-poor/Cr-free garnet + clinopyroxene assemblages. These metasomatic garnets with high Ca and very low Cr contents may be indistinguishable in terms of major elements from those in bimineralic 'Type C' eclogites, long hypothesized to be products of interaction of asthenosphere-derived melt and the base of cratonic lithosphere[27]. While the mineralogy, elemental and isotopic composition of Type C eclogites clearly indicate a low-pressure protolith[22], our experiments demonstrate that garnet with major-element compositions similar to Type C eclogites can be produced by deep metasomatic processes. Redox freezing of carbonated silicate melt may provide a mechanism for the formation of olivine-bearing as well as exotic wehrlitic rocks, but as the result of incipient melts and not major plume-related melting[27].

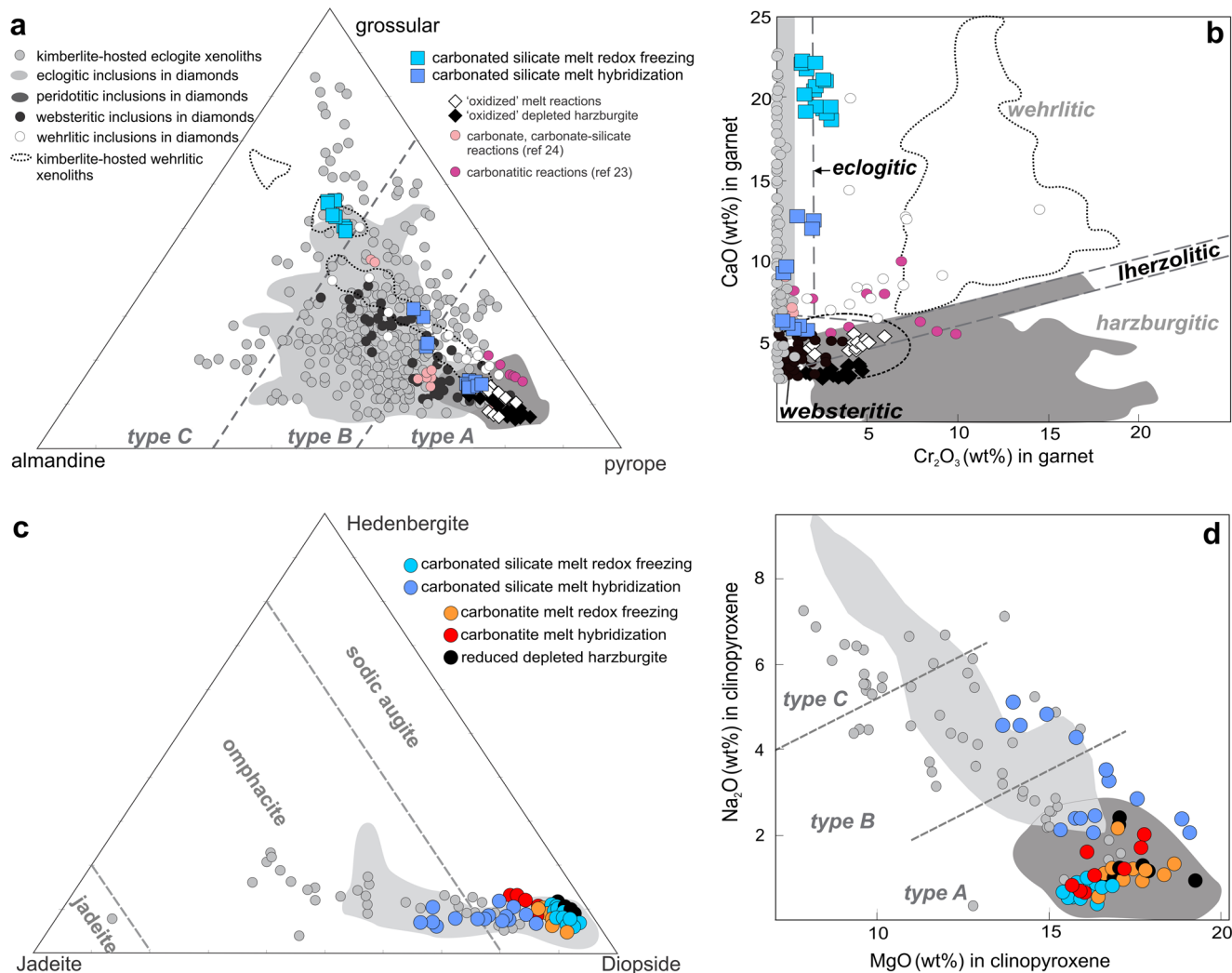**Redox fractionation zone.** Redox freezing and diamond deposition did not consume all the original melt in the

Fig. 4 Mineral compositions from reaction experiments. a Compositional diagram for garnet end-members almandine, pyrope, and grossular. Garnets from redox freezing and hybridization zones resulting from a carbonated silicate melt. **b** Cr_2O_3 vs. CaO (wt%) garnet discrimination diagram[49,50]. **c** Hedenbergite, jadeite, and diopside components in clinopyroxenes from experiments with carbonatite and carbonated silicate melts. **d** MgO vs. Na_2O content in clinopyroxene with fields for type A–C eclogites[51]. Blue and dark blue symbols are experimental garnets (squares) and clinopyroxenes (circles) from redox freezing and hybridization zones; diamond symbols are garnets from oxidized reaction experiments. Wehrlitic garnets in diamonds and kimberlite-hosted xenoliths[9,25,41], eclogitic garnets, peridotitic garnet inclusions in diamonds[13,22,41], websteritic[41] garnet inclusions in diamonds. Garnet compositions from previous experiments[20,21] (see key at top).

experiments, which evolved to a residual hydrous silica-poor liquid that is poorer in carbon. In both the carbonatite and carbonated silicate melt experiments, the reduction of the carbonate component of the melts to graphite in the "redox freezing zone" must have been accompanied by oxidation of some Fe^{2+} in the melts to Fe^{3+} and the release of H_2O, a trace fraction of which would have been incorporated into nominally anhydrous silicate minerals and minor phlogopite, with the majority dissolved in the evolving melt (Reaction (3))

$$4Fe^{2+} + CO_3^{2-} + 6\,H^+ = C + 3H_2O + 4Fe^{3+} \qquad (3)$$
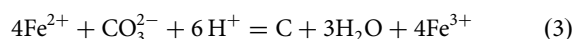
We infer that some of the Fe^{3+} were incorporated in the residual melt, which further infiltrated the depleted, reduced harzburgite in the capsule above the redox freezing zone. This evolved melt behaves as a metasomatic agent in the ensuing *redox fractionation zone* (Fig. 2), whereby Fe^{3+} in the melt is reduced to Fe^{2+} in an inverse Fe disproportion reaction (Reaction (4))

because the sample is buffered to $fO_2 \approx$ IW by the Fe capsule.

$$2Fe^{3+} + Fe = 3Fe^{2+}$$
$$Melt + capsule = olivine \qquad (4)$$
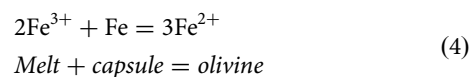
This in turn results in the formation of Fe-richer rims (90.3–93.1 Mg#) on olivines, partly replacing the rims of the original, high-Mg# olivines (95.2–97.8 Mg#) (Fig. 3). Accompanying the compositional change in the olivines, orthopyroxene and any clinopyroxene from the original harzburgite dissolved in the hydrous melt (Reaction (3)), leaving a spinel dunite residue (Fig. 2). Carbon in the melt was deposited as graphite (reaction (3) above), but is less common in the redox fractionation zone than in the initial redox freezing zone because of the previous deposition of graphite in the latter zone (Reactions (1) and (2)). This would have led to further Fe^{2+} production by reduction of Fe^{3+}, contributing to the Fe-rich olivine rims.

Olivine in the reduced experiments exhibits slightly higher Mg numbers than typically observed in cratonic lithospheric mantle, because of the buffering of the system to low fO_2 ($\approx$IW) by the Fe

capsules; a realistic natural range of Mg# in deep cratonic mantle lithosphere would be 92–94[28]. Nevertheless, the experiments replicate the broad style of metasomatism caused by reactive low-silica hydrous melts in the deep cratonic lithospheric mantle. Metasomatic olivine precipitated from hydrous melt in this way may possess elevated H_2O content, despite bearing the Mg# associated with geochemical depletion (90.3–93.1 Mg#, Fig. 3). This depleted chemical signature coupled with elevated H_2O content has been observed in cratonic peridotites sourced from ~4-5 GPa from the Siberian[29] and the Kaapvaal cratons[30,31].

The wide range of olivine compositions in the redox fractionation zone in these experiments resembles the variety of olivine compositions observed in lithospheric diamond inclusions[18,32,33] (Fig. 3). The present experiments thus suggest that some dunites and low-temperature harzburgites can be formed through infiltration by evolved hydrous, low-silica melts, and do not necessarily represent the residues of melting events[28,32]. These experimental results are analogous to the interpretation that dunite xenoliths with a range of Mg# may be produced by interaction with infiltrating "proto-kimberlitic" melts[34]. Low-pressure analogs of dunite formation by melt infiltration are well studied in ophiolites[35,36].

Hybridization zone. The *hybridization zone* refers to the leading edge of melt migration, where the melt finally solidifies, transforming the chemical components of the evolved melt into a new mineral assemblage. Through the redox fractionation zone, continued consumption of pyroxenes by the hydrous silica-poor melt increases the SiO_2 content of the melt and enriches it in alkalies, eventually resulting in the deposition of hydrous alkali-rich components in the hybridization zone in the case of the original alkali-rich carbonatite melt (Fig. 2—left, 2B, zone 3).

Reactions in the hybridization zone are strongly influenced by the original character of the incipient melt, which we illustrate by comparing the carbonatite and carbonated silicate reaction columns (Fig. 2).

Solidification of the carbonatite melts at the reaction front deposits a hydrous metasomatic assemblage containing clinopyroxene, phlogopite, K-richterite, and olivine, with minor orthopyroxene (Fig. 2 left). This hybridization zone resembles natural MARID (mica-amphibole-rutile-ilmenite-diopside) rocks, except for the lack of rutile and ilmenite, which may be attributable to the TiO_2-poor composition of the infiltrating carbonatite melt[14,37]. Natural cratonic MARID rocks generally lack carbon-bearing minerals, yet their origin has been linked to carbonate-bearing kimberlitic or lamproitic melts in uncertain ways[7,11]. Curious accessory minerals such as celestine and barite have been reported from MARID[38], consistent with the enrichment of incompatible elements such as Ba and Sr in evolved melts. Our reaction experiments illustrate a possible mechanism by which such rocks can form through hybridization reactions. Previous reaction experiments in oxidized conditions have produced a MARID-like assemblage from the reaction between kimberlite melt and peridotite[39], but in our experiments, the reduced peridotite behind the reaction front forms a direct association with the Fe-rich dunites and explains MARID assemblages as originating from an evolved melt. A sampling of MARID rocks from the deep cratonic roots is rare because these assemblages have lower melting points than peridotites[40], and so their components are usually to be found in the melts that bring other xenolith types to the surface. Any later heating at the base of the cratonic lithosphere would reactivate these hydrous mineral-rich layers (Fig. 1)[8,40].

Solidification of the carbonated silicate melt at the reaction front deposits Na-rich clinopyroxene, Mg-Ca-rich garnet, Fe-rich olivine (86.7–92.1 Mg#) and minor orthopyroxene (Fig. 2—right,

2C, zone 3). The lack of potassium in the carbonated silicate melt inhibits the crystallization of phlogopite. Garnet decreases in CaO, and Cr_2O_3 contents and increases in MgO as the reaction front progresses (Fig. 4A, B), whereas clinopyroxene decreases in MgO and increases in Na_2O content. The hybridization zone resembles natural diamond-bearing garnet clinopyroxenite-websterite assemblages with Mg–Ca-rich garnets and omphacitic clinopyroxenes (Fig. 4C, D).

Garnet clinopyroxenitic and websteritic garnet inclusions in lithospheric diamonds have similar major element characteristics as the experimental garnets from the hybridization zone[41]. This process could explain "mismatched" Mg-rich garnet and Na-rich clinopyroxene inclusions in lithospheric diamonds[42]. Our experiment describes a new mechanism where garnet-bearing clinopyroxenite- and websterite-like rocks could form by a hybridization reaction.

Conclusions

These redox reaction experiments demonstrate that several mineral assemblages known to occur in the cratonic lithosphere, but previously assumed to have unrelated origins, may be indeed be related and explained by the reaction of oxidized melts with reduced, depleted peridotites in conditions likely to correspond to cratonic roots. They demonstrate that diamonds could be deposited from carbonate-rich melts, enriching the melt in H_2O, alkalies, and silica, and explaining Fe-rich dunites and MARID-like assemblages as consecutive results of a single process. This also provides an alternative mechanism to subducted[22] or delaminated[43] crust, or underplating by voluminous silicate magmas[27] for the formation of pyroxenitic garnet and clinopyroxene inclusions in some lithospheric diamonds[19,41].

Methods

Experimental setup. Experiments were conducted in the high-pressure piston-cylinder apparatus at the Research School of Earth Sciences, Australian National University, Canberra (ANU), at a temperature of 1150 °C and pressure of 5 GPa for 12–24 h (Suppl. Table 2). NaCl cells with pyrex and MgO inserts were used as pressure media, a sintered Al_2O_3 cylinder as capsule holder, and graphite cylinders for heaters. Temperatures were monitored with B-type thermocouples (with no correction for the effect of pressure on the thermocouple electromotive force) and were controlled to within ±2 °C of the set point using a Eurotherm controller. Experiments were conducted with the hot piston-in technique. See further experimental details in Supplementary Notes 1 and 2.

After the experiments, capsules were embedded separately in epoxy mounts, and ground and polished under petroleum ether, avoiding contact with water to eliminate the possible dissolution of any alkali phases or quenched melts[13,14]. Once the capsules were breached, epoxy was drawn into the charge to minimize the loss of minerals and quenched melts during polishing. Samples UHP-435 and UHP-436 were repolished after analysis for ~2 h using colloidal silica suspension to remove the carbon coating and expose a new top layer for Raman measurements.

Analytical techniques. Analyses of solid phases and element maps were obtained by electron microprobe JEOL 8530 F Plus at 15 kV at the Center of Advanced Microscopy, ANU (Canberra), with a focused beam. Furthermore, X-ray maps of K, Na, Ca, Al, Si, Mg, Fe, and Cr were obtained with 0.5 μm grid spacing. Major elements of the melts were analyzed by JEOL 8530 F Plus electron microprobe operating at 15 kV and 3 nA, and additionally with a calibrated FE-SEM (Hitachi 4300 SE/N Schottky Field Emission) operated at 6 kV and 3 nA at Center of Advanced Microscopy (ANU, Canberra). Detection limits are 57–203 ppm (Si: 203 ppm, Ti: 118 ppm, Al: 131 ppm, Fe: 141 ppm, Mn: 145 ppm; Mg: 149 ppm; Ca: 78 ppm; Na: 144 ppm; K: 57 ppm; Cr: 157 ppm).

Raman spectroscopic measurements were performed at the School of Chemistry, Monash University (Melbourne) using a WITec® alpha300R Raman spectrometer with 532 nm laser excitation, and 3.85 mW laser energy. Analytical settings included 10× accumulations, 1 μm spot size, and 50× objective. Peaks were compared with those indicated in the literature as graphite and amorphous carbon[44,45].

Data availability

Underlying data for the main manuscript figures is included as excel files in Supplementary Data 1–5 (https://doi.org/10.26180/21547653). Further datasets are cited in the appropriate sections of the paper text and Supplementary Information.

References

1. Pearson, D. G. et al. Deep continental roots and cratons. *Nature* **596**, 199–210 (2021).
2. Frost, D. J. & McCammon, C. A. The redox state of Earth's mantle. *Ann. Rev. Earth Planet. Sci.* **36**, 389–420 (2008).
3. Rehfeldt, T., Foley, S. F., Jacob, D. E., Carlson, R. W. & Lowry, D. Contrasting types of metasomatism in dunite, wehrlite and websterite xenoliths from Kimberley, South Africa. *Geochim. Cosmochim. Acta* **72**, 5722e5756 (2008).
4. O'Reilly, S. Y., Griffin W. L. Mantle metasomatism. in (eds Harlov, D. E., Austrheim, H.) *Metasomatism and the Chemical Transformation of Rock.* (Springer-Verlag, Heidleberg, 2013), 471–533. https://doi.org/10.1007/978-3-642-28394-9_12.
5. Ionov, D. A., Doucet, L. S., Xu, Y., Golovin, A. V. & Oleinikov, O. B. Reworking of Archean mantle in the NE Siberian craton by carbonatite and silicate melt metasomatism: evidence from a carbonate-bearing, dunite-to-websterite xenolith suite from the Obnazhennaya kimberlite. *Geochim. Cosmochim. Acta* **224**, 132–153 (2018).
6. Simon, N. S. C., Carlson, R. W., Pearson, D. G. & Davies, G. R. The origin and evolution of the Kaapvaal cratonic lithosphere mantle. *J. Petrol.* **48**, 589–625 (2007).
7. Fitzpayne, A., Giuliani, A., Hergt, J., Phillips, D. & Janney, P. New geochemical constraints on the origins of MARID and PIC rocks: implications for mantle metasomatism and mantle-derived potassic magmatism. *Lithos* **318-319**, 478–493 (2018).
8. Foley, S. F. Rejuvenation and erosion of the cratonic lithosphere. *Nat. Geosci.* **1**, 503–510 (2008).
9. Aulbach, S., Lin, A.-B., Weiss, Y. & Yaxley, G. M. Wehrlites from continental mantle monitor the passage and degassing of carbonated melts. *Geochem. Perspect. Lett.* **15**, 30–34 (2020).
10. Gregoire, M., Bell, D. R. & Le Roex, A. P. Trace element geochemistry of phlogopite-rich mafic mantle xenoliths: their classification and their relationship to phlogopite-bearing peridotites and kimberlites revisited. *Contribut. Mineral. Petrol.* **142**, 603–625 (2002).
11. Waters, F. G. A suggested origin of MARID xenoliths in kimberlites by high pressure crystallization of an ultrapotassic rock such as lamproite. *Contribut. Mineral. Petrol.* **95**, 523–533 (1987).
12. Foley, S. F., Pintér, Z. Primary melt compositions in the Earth's mantle. in (eds Kono, Y. & Sanloup, C.) *Magmas under Pressure: Advances in High-Pressure Experiments on Structure and Properties of Melts.* (Elsevier, Amsterdam, 2018) 3-42. https://doi.org/10.1016/B978-0-12-811301-1.00001-0.
13. Pintér, Z. et al. Experimental investigation of the composition of incipient melts in upper mantle peridotites in the presence of CO_2 and H_2O. *Lithos* **396**, 106224 (2021).
14. Foley, S. F. et al. The composition of near-solidus melts of peridotite in the presence of CO_2 and H_2O at 40 – 60 kbar. *Lithos* **112S**, 274–283 (2009).
15. Brey, G. P., Bulatov, V. K. & Girnis, A. V. Melting of K-rich carbonated peridotite at 6-10 GPa and the stability of K-phases in the upper mantle. *Chem. Geol.* **281**, 333–342 (2011).
16. Foley, S. F. A reappraisal of redox melting in the Earth's mantle as a function of tectonic setting and time. *J. Petrol.* **52**, 1363e1391 (2011).
17. Rohrbach, A. & Schmidt, M. W. Redox freezing and melting in the Earth's deep mantle resulting from carbon-iron redox coupling. *Nature* **472**, 209–212 (2011).
18. Stachel, T. & Luth, R. W. Diamond formation—where, when and how? *Lithos* **220-223**, 200–220 (2015).
19. Shirey, S. B. et al. Diamonds and the geology of mantle carbon. *Rev. Mineral. Geochem.* **75**, 355–421 (2013).
20. Sokol, A. G., Kruk, A. N., Chebotarev, D. A. & Palyanov, Y. N. Carbonatite melt/peridotite interaction at 5.5-7 GPa: implications for metasomatism in Lithospheric mantle. *Lithos* **248-251**, 66–79 (2016).
21. Gervasoni, F., Klemme, S., Rohrbach, A., Grutzner, T. & Berndt, J. Experimental constrains on mantle metasomatism caused by silicate and carbonate melts. *Lithos* **282-283**, 173–186 (2017).
22. Jacob, D. E. Nature and origin of eclogite xenoliths from kimberlites. *Lithos* **77**, 295–316 (2004).
23. Shatskiy, A., Bekhtenova, A., Podbodnikov, I. V., Arefiev, A. V. & Litasov, K. D. Towards composition of carbonatite melts in peridotitic mantle. *Earth Planet. Sci. Lett.* **581**, 117395 (2022).
24. Aulbach, S. et al. Ultramafic carbonated melt-and auto-metasomatism in mantle eclogites: compositional effects and geophysical consequences. *Geochem. Geophys. Geosyst.* **21**, e2019GC008774 (2020).
25. Sobolev, N. V., Lavrent'Ev, Y. G., Pokhilenko, N. P. & Usova, L. V. Chrome-rich garnets from the kimberlites of Yakutia and their parageneses. *Contrib. Mineral. Petrol.* **40**, 39–52 (1973).
26. Kopylova, M. G., Russell, J. K. & Cookenboo, H. Petrology of peridotite and pyroxenite xenoliths from the Jericho kimberlite: implications for the thermal state of the mantle beneath the Slave craton, northern Canada. *J. Petrol.* **40**, 79–104 (1999).
27. Griffin, W. L. & O'Reilly, S. Y. Cratonic lithospheric mantle: is anything subducted? *Episodes* **30**, 43–53 (2007).
28. Griffin, W., O'Reilly, S. Y., Afonso, J. C. & Begg, G. The composition and evolution of lithospheric mantle: a re-evaluation and its tectonic implications. *J. Petrol.* **50**, 1185–1204 (2009).
29. Doucet, L. S. et al. High water content in the Siberian cratonicmantle linked to melt metasomatism: an FTIR study of Udachnaya peridotite xenoliths. *Geochim. Cosmochim. Acta* **137**, 159–187 (2014).
30. Jones, A. G., Fishwick, S., Evans, R. L., Muller, M. R. & Fullea, J. Velocity-conductivity relations for cratonic lithosphere and their application: example of Southern Africa. *Geochem. Geophys. Geosyst.* **14**, 806–827 (2013).
31. Peslier, A. H., Woodland, A. B., Bell, D. R., Lazarov, M. & Lapen, T. J. Metasomatic control of water contents in the Kaapvaal cratonic mantle. *Geochim. Cosmochim. Acta* **97**, 213–246 (2012).
32. Pearson, D. G. & Wittig, N. The formation and evolution of cratonic mantle lithosphere—evidence from mantle xenoliths. in (eds Holland, H. D., Turekian, K. K.), *Treatise on Geochemistry.* (Elsevier Ltd., Amsterdam, 2014) 255–292.
33. Agashev, A. M. et al. Metasomatism in lithospheric mantle roots: constraints from whole-rock and mineral chemical composition of deformed peridotite xenoliths from kimberlite pipe Udachnaya. *Lithos* **160**, 201–215 (2013).
34. Rooney, T. O., Girard, G. & Tappe, S. The impact on mantle olivine resulting from carbonated silicate melt interaction. *Contrib. Mineral. Petrol.* **175**, 1–15 (2020).
35. Kelemen, P. B. Reaction between ultramafic rock and fractionating basaltic magma. I. Phase relations, the origin of calc-alkaline magma series, and the formation of discordant dunite. *J. Petrol.* **31**, 51–98 (1990).
36. Daines, M. J. & Kohlstedt, D. L. The transition from porous to channelized flow due to melt/rock reaction during melt migration. *Geophys. Res. Lett.* **21**, 145–148 (1994).
37. Kargin, A. V. Titanium-rich metasomatism in the lithospheric mantle beneath the Arkhangelsk Diamond Province, Russia: insights from ilmenite-bearing xenoliths at H-HT reaction experiments. *Contrib. Mineral. Petrol.* **176**:101. https://doi.org/10.1007/s00410-021-01863-9 (2021).
38. Giuliani, A. et al. Mantle oddities: a sulphate fluid preserved in a MARID xenolith from the Bultfontein kimberlite (Kimberley, South Africa). *Earth Planet. Sci. Lett.* **376**, 74–86 (2013).
39. Odling, N. W. A. An experimental replication of upper-mantle metasomatism. *Nature* **373**, 58–60 (1995).
40. Foley, S., Musselwhite, D., & van der Laan, S. R. Melt compositions from ultramafic vein assemblages in the lithospheric mantle: a comparison of cratonic and non-cratonic settings. in (ed J. J. Gurney), *Proceedings of the 7th International Kimberlite Conference.* Vol. 1. (Red Roof Design, Cape Town 1999) 238–246.
41. Stachel, T. & Harris, J. W. The origin of cratonic diamonds—constraints from mineral inclusions. *Ore Geol. Rev.* **34**, 5–32 (2008).
42. Wang, W. Formation of diamond with metal mineral of 'mixed' eclogite and peridotite paragenesis. *Earth Planet. Sci. Lett.* **160**, 831–843 (1998).
43. Le Roux, A., Tinguely, C. & Gregoire, M. Eclogite and garnet pyroxenite xenoliths from kimberlites emplaced along the southern margin of the Kaapvaal craton, southern Africa: mantle or lower crustal fragments? *J. Petrol.* **61**, egaa040 (2020).
44. Tuinstra, F. & Koenig, J. L. Raman spectrum of Graphite. *J. Chem. Phys.* **53**, 1126–1130 (1970).
45. Kalish, R., Reznik, A., Nugent, K. W. & Prawer, S. The nature of damage in ion-implanted and annealed diamond. *Nuclear Instruments and Methods in Physics research Section B: Beam Interactions with Materials and Atoms* **148**, 626–633 (1999).
46. Day, H. W. A revised diamond-graphite transition curve. *Am. Mineral.* **97**, 52–62 (2012).
47. Yaxley, G. M., Berry, A. J., Kamenetsky, V. S., Woodland, A. B. & Golovin, A. V. An oxygen fugacity profile through the Siberian Craton—Fe K-edge XANES determinations of Fe3+/sigma Fe in garnets in peridotite xenoliths from the Udachnaya East kimberlite. *Lithos* **140**, 142–151 (2012).
48. Pollack, H. N. & Chapman, D. S. On the regional variation of heat flow, geotherms, and lithospheric thickness. *Tectonophysics* **38**, 279–296 (1977).
49. Grütter, H. S., Gurney, J. J., Menzies, A. H. & Winter, F. An updated classification scheme for mantle-derived garnet, for use by diamond explorers. *Lithos* **77**, 841–857 (2004).

50. Coleman, R. G., Lee, D. E., Beatty, L. B. & Brannock, W. W. Eclogites and eclogites: their differences and similarities. *Geol. Soc. Amer. Bull.* **76**, 483–508 (1965).
51. Taylor, L. A. & Neal, C. R. Eclogites with oceanic crustal and mantle signatures from the Bellsbank kimberlite, South Africa, Part I: mineralogy, petrography, and whole rock chemistry. *J. Geol.* **97**, 551–567 (1989).

Author contributions

Z.P.: methodology, validation, investigation, formal analysis, visualization, writing—original draft, writing—review and editing. S.F.F.: conceptualization, supervision, validation, resources, funding acquisition, writing—review and editing. G.M.Y.: conceptualization, supervision, validation, resources, writing—review and editing.

Competing interests

The authors declare no competing interests.

Additional information

Supplementary information The online version contains supplementary material available at https://doi.org/10.1038/s43247-022-00630-3.

Correspondence and requests for materials should be addressed to Zsanett Pintér.

Peer review information *Communications Earth & Environment* thanks Sonja Aulbach, Sebastian Tappe, and the other, anonymous, reviewer(s) for their contribution to the peer review of this work. **Primary Handling Editors**: Maria Luce Frezzotti, Joe Aslin, Clare Davis. Peer reviewer reports are available.

Reprints and permission information is available at http://www.nature.com/reprints

Publisher's note Springer Nature remains neutral with regard to jurisdictional claims in published maps and institutional affiliations.